Desalination and Water Treatment
www.deswater.com

doi: 10.5004/dwt.2017.20940

90 (2017) 16–22
September

Prediction of silica fouling using mathematical model and artificial neural network in a direct contact membrane distillation

Yongjun Choi, Yongsun Jang, Sangho Lee*

School of Civil and Environmental Engineering, Kookmin University, Jeongneung-dong, Seongbuk-Gu, Seoul 136-702, Korea, Tel. +82-2-910-4529; Fax: +82-2-910-4939; email: sanghlee@kookmin.ac.kr (S. Lee)

Received 1 February 2017; Accepted 5 May 2017

ABSTRACT

Membrane distillation (MD) is an emerging alternative to conventional desalination technologies such as reverse osmosis and distillation. However, the critical problem of membrane fouling must be resolved if MD technology is to find widespread applications. Such fouling reduces the flux and increases energy consumption. In this study, we investigated the colloidal silica fouling characteristics of a direct-contact membrane distillation system and the use of mathematical models and an artificial neural network (ANN) to predict the rate of fouling. The results showed that the flux was affected by the silica concentration, NaCl concentration, and feed temperature. A cake formation model was found to most accurately describe the colloidal silica fouling in MD under experimental conditions, with R^2 values between 0.93 and 0.99. This suggests that the main factor in colloidal silica fouling is the buildup of a cake layer at the membrane surface. The results from the ANN model indicated high correlation ($R^2 = 0.99$) between the experimentally measured and predicted output variables. This confirmed the ability of the ANN model to accurately predict the rate of silica fouling in an MD system.

Keywords: Membrane distillation; Fouling; Silica; Model; Artificial neural network

1. Introduction

Water scarcity is becoming one of the main problems faced by many countries around the world [1,2]. The availability of clean water is crucial to the development of human society [3], and countries are therefore seeking alternative sources. Among these, seawater desalination has been shown to be a reliable and economically sustainable source [4].

An emerging approach to seawater desalination is the use of membrane distillation (MD). MD is a thermal process in which separation is driven by the vapor pressure resulting from a temperature gradient created across a microporous hydrophobic membrane. This causes the water and volatile compounds on the hot side to evaporate and migrate through the pores, finally condensing on the permeate side [5]. MD has several advantages over reverse osmosis (RO) and other desalination methods. MD can completely remove the ions, dissolved non-volatile organics, colloids, and pathogenic microorganisms that may be present in the feed solution [6–8]. More importantly, owing to the discontinuity of the liquid phase across the membrane, MD can be used to treat highly saline water [7].

However, MD is still in the early stage of commercial development [9]. A major challenge is membrane fouling, which decreases the separation efficiency and increases the energy demand, and therefore the cost [10]. Fouling in MD is less understood than that in RO. Because of differences in membrane structure and operating conditions, the fouling mechanisms in MD are expected to be different from those encountered in RO or nanofiltration [11]. Few studies have addressed the effects of temperature, pH, flow rate, and other factors such as ionic strength and the co-existence of certain ions on the silica fouling found in MD [12–15].

* Corresponding author.

Presented at the 9th International Desalination Workshop: Sustainable Desalination (IDW2016), 13–15 November 2016, Abu Dhabi, UAE.

Colloidal particulates are ubiquitous in natural waters and range in size from 1 to 1,000 nm [16]. Removal of particles smaller than 1,000 nm has been reported to be ineffective in avoiding fouling [17]. In the neutral-pH range typical of natural water bodies, the surface of most colloids has a negative charge, reflecting the surface chemical properties and chemical composition of natural waters [18]. In membrane fouling, opposite charges cause these colloids to accumulate on the membrane surface or within the membrane pores, adversely affecting the permeate flux and solute concentration of the output water [19].

This study investigated colloidal silica fouling in a direct-contact MD (DCMD) system. A cake formation model was developed to predict the rate of fouling, and an artificial neural network (ANN) was constructed. The role of the colloidal silica concentration, feed temperature, and NaCl concentration on fouling was also clarified.

2. Theoretical background

2.1. Mathematical model

Since microporous membranes are used in MD, silica fouling may occur due to formation of a cake layer on the membrane surface as well as due to the deposition of silica particles within the pore/support layer. Mathematical models are therefore needed to identify the principal mechanisms of silica fouling and to predict the rate of fouling. In this study, three membrane-fouling models were developed based on the blocking filtration laws modified for application to the crossflow filtration mode [20]: a pore blocking model, a pore constriction model, and a cake formation model (Table 1). Pore blocking and constriction are fouling mechanisms internal to the membrane, whereas cake formation occurs on the surface and is therefore defined as external fouling. The predictions made by the models were tested by applying the R^2 criterion. Using experimental data, the minimum R^2 values from the three models were compared to determine the principal fouling mechanism.

2.2. ANN model

While mathematical models can be used to analyze fouling characteristics, they are of limited use in predicting the progress of fouling, given the complexity of the factors involved. An ANN model was therefore used to understand and predict the course of fouling. An ANN is a computational model that can simulate the processing and learning functions of the human brain [21]. It comprises a group of parallel processing elements called neurons organized as units of knots [21]. Neurons in each layer of the ANN are connected to those in the adjoining layer by a number of weighted connections. An extra weight, called bias, is added to the other input weights [21]. An ANN is trained to learn a particular function by adjusting the weights applied to the connections until the network output matches the target. This allows the network to predict the correct outputs from a given set of inputs. The basic component of an ANN is the node (or neuron). Fig. 1 shows a single node of an ANN. Inputs are labeled x_1, x_2, and x_i, and the output is labeled y_j. Each node may receive multiple input signals. The node manipulates the inputs to produce a single output. The strength of each connection, referred to as its connection weight, reflects adaptive coefficients within the network that determine the intensity of the input signal. Input data are presented to the network through the input layer, the values of which are denoted by x_i. Each input is multiplied by its corresponding weight and the node uses the sum of these weighted inputs ($W_{ij} \times x_1$) to produce an output signal, by applying a transfer function. These weighted inputs are then summed and added to a threshold value (θ_j) to produce the net node input (I_j). This is done using the following equation:

$$I_j = \Sigma_{i=1}^{n}(W_{ij} \times x_i) + \theta_j \quad (1)$$

The output of a node is determined by performing a mathematical operation on the net input to the node. This is called the transfer function, and it can transform the net input in a linear or non-linear manner. Three types of transfer functions are commonly used.

The sigmoid transfer function:

$$f(I_j) = \frac{1}{1+e^{-I}} \; (0 < f(I) < 1) \quad (2)$$

The hyperbolic tangent transfer function:

$$f(I_j) = \tanh(\mathrm{I}) = \frac{e^{I} - e^{-I}}{e^{I} + e^{-I}} \; (-1 < f(I) < 1) \quad (3)$$

Table 1
Fouling models

Fouling type	Equation
Pore constriction model	$\sqrt{\frac{J_0}{J}} - 1 = Kt$
Pore blocking model	$\ln\left(\frac{J_0}{J}\right) = Kt$
Cake formation model	$\left(\frac{J_0}{J}\right)^2 - 1 = Kt$

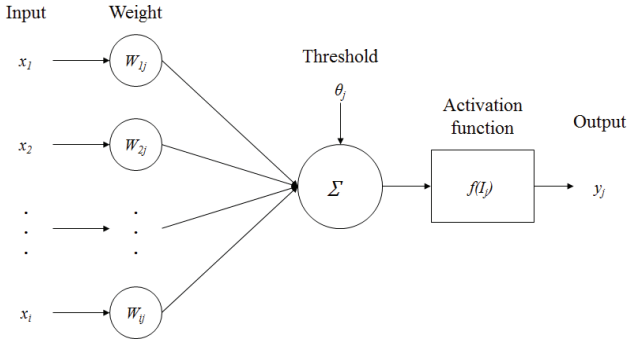

Fig. 1. Schematic diagram of a single node structure.

The linear transfer function:

$$f(I_j) = I \ (-\infty < f(I) < \infty) \tag{4}$$

The net node input (I_j) is then passed through an activation function to produce the node output, y_j, which is then used to compute the inputs to the nodes in the higher layer, until the final output is derived [22].

In this study, a multilayer feedforward neural network trained by a back-propagation algorithm was used. Fig. 2 shows a fully connected multilayer perceptron (MLP). An MLP has three or more layers of nodes: an input layer, an output layer, and one or more hidden layers. MLPs are widely used in research owing to their ability to solve problems stochastically, which often enables obtaining approximate solutions for highly complex problems such as fitness approximation.

3. Materials and methods

3.1. Colloidal silica

Colloidal silica (SNOWTEX, Nissan Chemical (Tokyo, Japan)) with an average diameter of 70–100 nm was used as a model colloidal foulant. Spherical and mono-disperse colloidal suspensions were created in water. The particles were supplied as a stable concentrated aqueous suspension at an alkaline pH of between 8.5 and 9.5. The concentrated stock suspension was stored at 4°C. Prior to use, it was hand-shaken and then sonicated for at least 30 min to thoroughly disperse the silica particles. Silica concentrations of 3,000 and 7,000 mg/L and NaCl concentrations of 15,000 and 30,000 mg/L were used. To allow the effect on MD fouling of the colloidal silica concentration, NaCl concentration, and feed temperature to be disaggregated, four different test conditions were used (listed in Table 2). All fouling tests were conducted for 9 h using 2 L of feedwater in each case.

3.2. Experimental setup

Fig. 3 shows a schematic diagram of the MD filtration device used in this study. This was a DCMD system with a plate and frame module. In this system, a hydrophobic porous membrane separated the hot feed from the cold distillate. At the membrane interface, the water evaporated on the hot side, diffused through the membrane pores, and condensed at the membrane interface on the cold side. A commercially available flat sheet MD membrane with a nominal pore size of 0.22 μm (Merck Millipore, Billerica, USA) was used. Table 3 gives the specifications of the membrane. The flow rates of the feed and permeate were, respectively, set at 0.6 and 0.4 L/min using a gear pump. The feed temperatures were 60°C and 70°C, while a temperature control unit maintained the cold permeate water at 20°C.

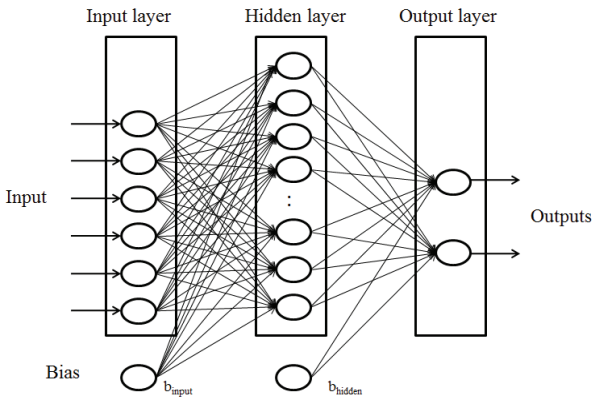

Fig. 2. Schematic diagram of a multilayer feedforward neural network.

4. Results and discussion

4.1. Effect of colloidal silica concentration

First, the effect of colloidal silica concentration on MD fouling was investigated. The results are shown in Fig. 4. Silica concentrations of 3,000 mg/L (Case 1) and 7,000 mg/L (Case 2) were used, and all other experimental conditions including feed/distillate temperature, feed salt concentration, and feed/distillate flow rate were held constant. As expected, a relationship was found between the colloidal silica concentration and the rate of fouling. Although the initial flux was

Table 2
Experimental conditions

	Silica concentration (mg/L)	NaCl concentration (mg/L)	Feed temperature (°C)
Case 1	3,000	30,000	60
Case 2	7,000	30,000	60
Case 3	7,000	15,000	60
Case 4	7,000	30,000	70

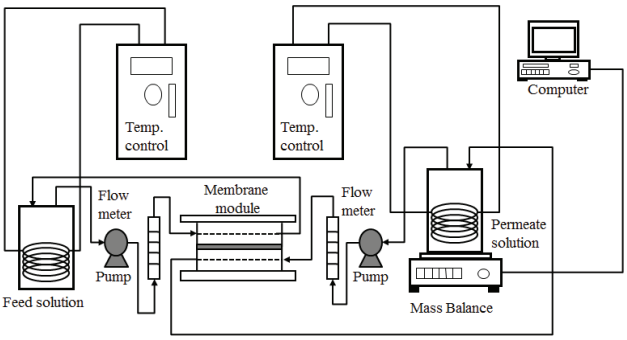

Fig. 3. Schematic diagram of MD experimental setup.

Table 3
Specifications of the MD membrane

Material type	PVDF
Area of module	12 cm^2
Porosity	75%
Thickness	125 μm
Pore size	0.22 μm
Contact angle	130°

not affected by the silica concentration, the rate at which it declined was higher at the higher concentration. After 9 h of MD operation, the flux value reduced to 59% of its initial rate at a silica concentration of 3,000 mg/L and to 43% at a concentration of 7,000 mg/L.

4.2. Effect of NaCl concentration

Next, the effect of the NaCl concentration on MD silica fouling was investigated using a silica concentration of 7,000 mg/L and NaCl concentrations of 30,000 mg/L (Case 2) and 15,000 mg/L (Case 3). The results are shown in Fig. 5. The NaCl concentration had little effect on the initial flux.

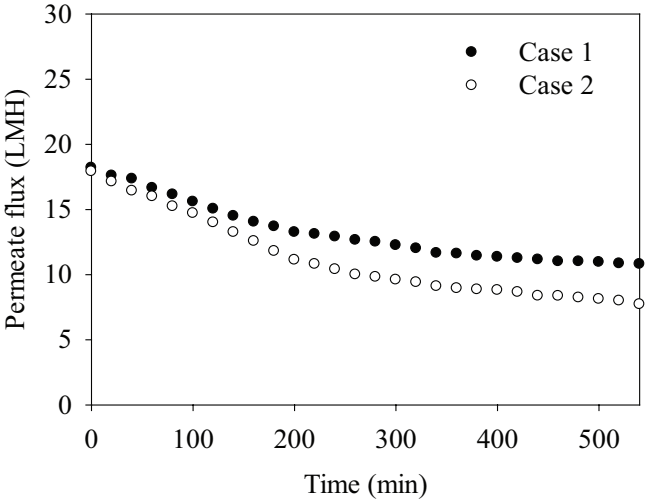

Fig. 4. MD flux levels for different colloidal silica concentrations with respect to time. Case 1: silica concentration 3,000 mg/L; NaCl concentration 30,000 mg/L; temperature 60°C. Case 2: silica concentration 7,000 mg/L; NaCl concentration 30,000 mg/L; temperature 60°C.

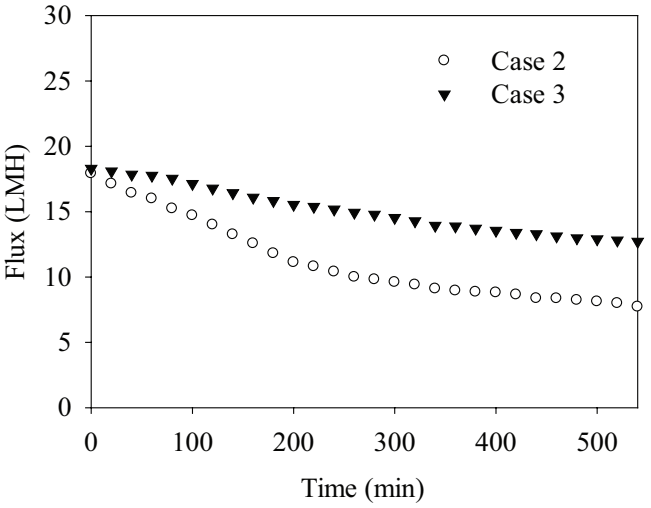

Fig. 5. MD flux levels for different NaCl concentrations with respect to time. Case 2: silica concentration 7,000 mg/L; NaCl concentration 30,000 mg/L; temperature 60°C. Case 3: silica concentration 7,000 mg/L; NaCl concentration 15,000 mg/L; temperature 60°C.

This is because MD is less sensitive than RO to the salt concentration in the feed. However, the rate of decline in flux was higher in Case 2 than Case 3. This suggested that while NaCl is not itself a foulant, it accelerated the colloidal fouling in the MD membrane. After 9 h of MD operation, the flux value reduced to 69% of its initial rate at an NaCl concentration of 15,000 mg/L and to 43% at a concentration of 30,000 mg/L.

4.3. Effect of feed temperature

The effect of the feed temperature on MD fouling is shown in Fig. 6. The feed temperatures were 60°C (Case 2) and 70°C (Case 4), with all other experimental conditions including silica concentration, permeate temperature, feed salt concentration, and feed/distillate flow rate held constant. The decline in flux was linear at 60°C, but a much faster initial rate of decline was observed at 70°C. The initial flux was higher at 70°C than at 60°C, because the driving force of MD is temperature-dependent. However, after 110 min, the flux at 70°C converged to that at 60°C, suggesting that initial fouling was more rapid at the higher temperature. After 9 h of MD operation, the flux value reduced to 43% of its initial rate at 60°C and to 27% at 70°C.

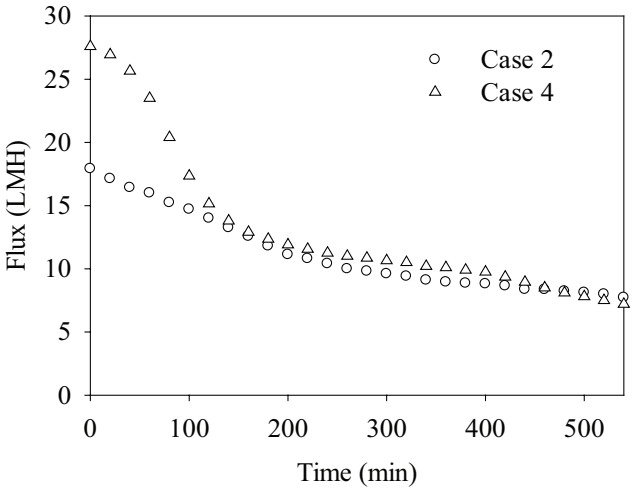

Fig. 6. MD flux levels for different feed temperatures with respect to time. Case 2: silica concentration 7,000 mg/L; NaCl concentration 30,000 mg/L; temperature 60°C. Case 4: silica concentration 7,000 mg/L; NaCl concentration 30,000 mg/L; temperature 70°C.

Table 4
Comparison of model parameters for each filtration model

Case	Pore constriction model		Pore blocking model		Cake formation model	
	K	R^2	K	R^2	K	R^2
Case 1	0.00065	0.91	0.00116	0.88	0.00381	0.96
Case 2	0.00108	0.94	0.00180	0.90	0.00796	0.97
Case 3	0.00039	0.98	0.00073	0.97	0.00201	0.99
Case 4	0.00188	0.81	0.00283	0.90	0.02076	0.93

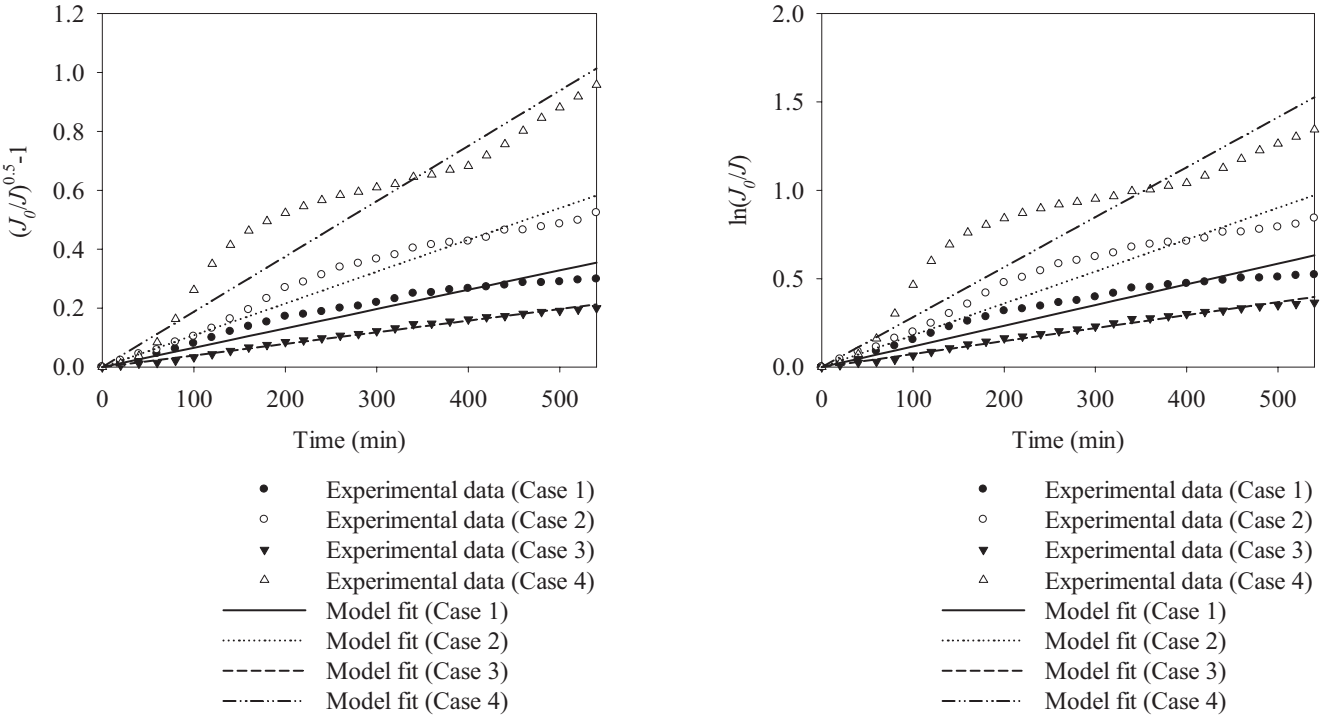

a) Pore constriction model

b) Pore blocking model

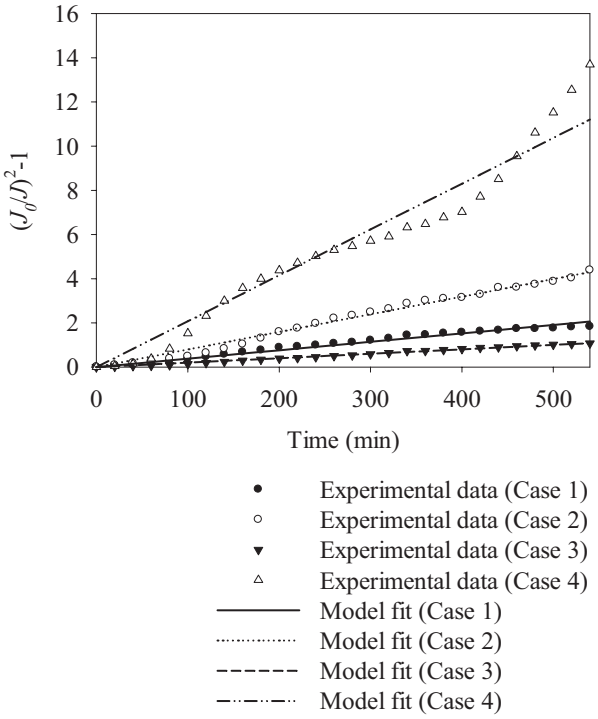

c) Cake formation model

Fig. 7. Comparison of model fit and experimental data. (a) Pore constriction model; (b) pore blocking model; and (c) cake formation model.

4.4. Model fitting using Hermia models

To further investigate the silica fouling characteristics of MD, three simple mathematical models (for pore blockage, pore constriction, and cake formation) were applied to the experimental data. The model fits of the different models are shown in Table 4. As can be seen from this table and Fig. 7, the cake formation model showed the highest level of agreement in all cases. This suggested that the main cause of colloidal silica fouling was the buildup of a cake layer at the membrane surface. The model parameter of the cake formation model, K, was calculated to fall between 0.00381 and 0.00210 h^{-1}, with an R^2 value of between 0.93 and 0.99.

Case 4 had the highest K value. This was attributed to the high initial flux produced by the high feed temperature, which accelerated the concentration polarization and produced an accumulation of colloidal silica in a mass transfer boundary layer adjacent to the membrane surface. The concentration polarization generally increases the level of fouling by increasing the concentration of contaminants near the membrane surface, which consequently aggravates the factors that cause fouling. This suggested that a denser cake layer was formed, increasing the K value. The lowest K value was recorded in Case 3. This can be explained by the effect of the cake layer on the vapor pressure near the membrane surface. A cake layer of colloidal silica can increase the concentration polarization by reducing the back-diffusion of salts near the membrane surface. The salt concentration is therefore higher in the cake layer than in the bulk solution, leading to a lower vapor pressure within the layer and at the membrane surface. The resulting reduction in the effective vapor pressure difference between the feed and distillate reduces the flux. This is similar to cake-enhanced osmotic pressure (CEOP) and can be referred to as cake-reduced vapor pressure (CRVP).

4.5. Model fitting using the ANN model

The ANN model was designed to simulate silica fouling in an MD system. The ANN model used in this study was created via MATLAB, as a platform for the simulation. The Network/Data Manager window in the MATLAB Toolbox allows the user to import, create, run, and export neural networks and data. The properties of the ANN model are shown in Table 5.

The application randomly divided the input vectors and target vectors into three sets: 70% for training, 15% for use in confirming that the network was generalizing and that training halted before over-fitting arose, and 15% to provide a completely independent test of network generalization. Fig. 8 compares the predicted flux levels and the experimental results as a function of the filtration time. The values predicted by the model matched the experimental values closely. The correlation coefficient (R) and mean squared error (MSE) were used to evaluate the performance of the ANN model.

Fig. 9 is a plot of the MSE against the number of iterations. A sharp drop in the MSE in the first few iterations (fast training) can be seen. The training cycle stopped after 33 iterations, and the smallest MSE value of 0.004 was recorded at 38 iterations.

Table 5
The properties of the ANN model

Network inputs	Filtration time, silica concentration, NaCl concentration, feed temperature
Network outputs	Permeate flux
Network type	Feed-forward back propagation
Training function	Levenberg–Marquardt
Performance function	Mean squared error
Number of hidden layers	1
Number of neurons in hidden layer	12

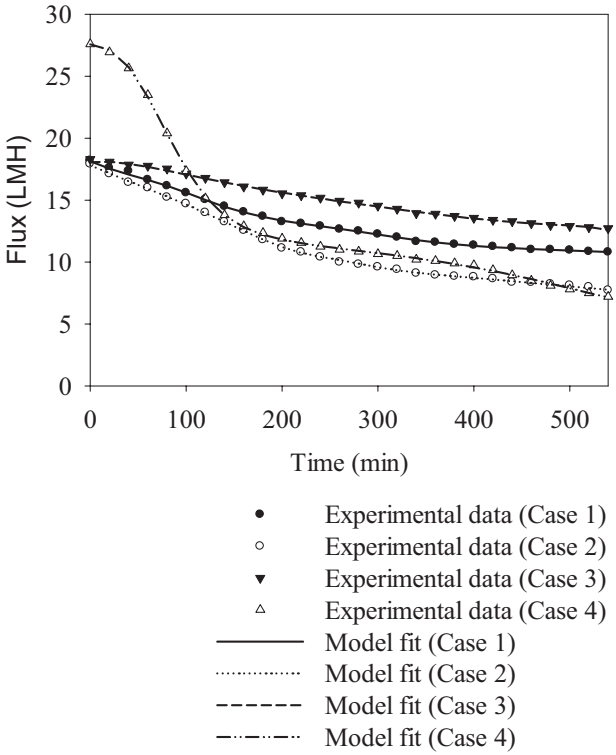

Fig. 8. Comparison of fit between the ANN model and the experimental data.

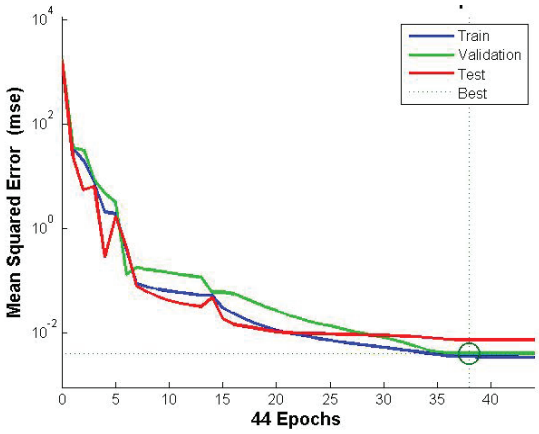

Fig. 9. MSE as a function of the number of iterations.

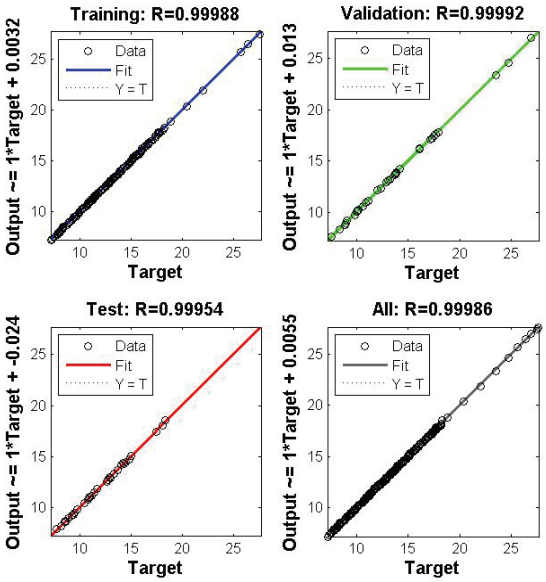

Fig. 10. ANN model regression for training, testing, validation, and all data.

The ANN model showed high strength, and a linear relationship was observed between the predicted results and the experimental data. The output tracked the targets very well for training (R value = 0.999), validation (R value = 0.999), and testing (R value = 0.999), as shown in Fig. 10. These values are equivalent to a total-response R value of 0.999, suggesting that the ANN model was able to predict all experimental cases simultaneously with very high accuracy.

5. Conclusions

In this study, colloidal silica fouling in an MD membrane was investigated using three simple mathematical fouling models and an ANN model. The following conclusions were drawn:

- The rate of permeate-flux decline due to silica fouling was influenced by the silica concentration, NaCl concentration, and feed temperature.
- A high concentration of salt accelerates colloidal fouling and flux decline. We attribute this to a reduction in the effective vapor pressure difference between feed and distillate and refer to this effect as CRVP.
- The cake formation model was found to give the most effective explanation of colloidal silica fouling. This suggests that cake formation is the dominant mechanism of fouling in an MD membrane by colloidal silica.
- When applying the ANN model, correlation coefficients of up to 0.99 were found between the measured and predicted output variables. Therefore, the ANN model accurately replicated the experimental data, suggesting that it can be used to predict silica fouling in a DCMD.

Acknowledgment

This research was supported by a grant (code 16IFIP-B065893-04) from Industrial Facilities & Infrastructure Research Program funded by Ministry of Land, Infrastructure and Transport of Korean government.

References

[1] Z. Zeng, J. Liu, H.H.G. Savenije, A simple approach to assess water scarcity integrating water quantity and quality, Ecol. Indic., 34 (2013) 441–449.
[2] L.A. Hoover, W.A. Phillip, A. Tiraferri, N.Y. Yip, M. Elimelech, Forward with osmosis: emerging applications for greater sustainability, Environ. Sci. Technol., 45 (2011) 9824–9830.
[3] M. Pedro-Monzonís, A. Solera, J. Ferrer, T. Estrela, J. Paredes-Arquiola, A review of water scarcity and drought indexes in water resources planning and management, J. Hydrol., 527 (2015) 482–493.
[4] C. Charcosset, A review of membrane processes and renewable energies for desalination, Desalination, 245 (2009) 214–231.
[5] M.S. El-Bourawi, Z. Ding, R. Ma, M. Khayet, A framework for better understanding membrane distillation separation process, J. Membr. Sci., 285 (2006) 4–29.
[6] K.W. Lawson, D.R. Lloyd, Membrane distillation, J. Membr. Sci., 124 (1997) 1–25.
[7] A.M. Alklaibi, N. Lior, Membrane-distillation desalination: status and potential, Desalination, 171 (2005) 111–131.
[8] L. Mariah, C.A. Buckley, C.J. Brouckaert, E. Curcio, E. Drioli, D. Jaganyi, D. Ramjugernath, Membrane distillation of concentrated brines – role of water activities in the evaluation of driving force, J. Membr. Sci., 280 (2006) 937–947.
[9] P. Wang, T.-S. Chung, Recent advances in membrane distillation processes: membrane development, configuration design and application exploring, J. Membr. Sci., 474 (2015) 39–56.
[10] M. Gryta, Fouling in direct contact membrane distillation process, J. Membr. Sci., 325 (2008) 383–394.
[11] A.K. Fard, T. Rhadfi, M. Khraisheh, M.A. Atieha, M. Khraisheha, N. Hilal, Reducing flux decline and fouling of direct contact membrane distillation by utilizing thermal brine from MSF desalination plant, Desalination, 379 (2016) 172–181.
[12] D. Singh, P. Prakash, K.K. Sirkar, Deoiled produced water treatment using direct-contact membrane distillation, Ind. Eng. Chem. Res., 52 (2013) 13439–13448.
[13] H.C. Duong, S.R. Gray, M. Duke, T.Y. Cath, L.D. Nghiem, Scaling control during membrane distillation of coal seam gas reverse osmosis brine, J. Membr. Sci., 493 (2015) 673–682.
[14] J. Gilron, Y. Ladizansky, E. Korin, Silica fouling in direct contact membrane distillation, Ind. Eng. Chem. Res., 52 (2013) 10521–10529.
[15] W. Zhong, H. Li, Y. Ye, V. Chen, Evaluation of silica fouling for coal seam gas produced water in a submerged vacuum membrane distillation system, Desalination, 393 (2016) 52–64.
[16] C.M. Law, X.-Y. Li, Q. Li, The combined colloid-organic fouling on nanofiltration membrane for wastewater treatment and reuse, Sep. Sci. Technol., 45 (2010) 935–940.
[17] X. Zhu, M. Elimelech, Colloidal fouling of reverse osmosis membranes: measurements and fouling mechanisms, Environ. Sci. Technol., 31 (1997) 3654–3662.
[18] W. Stumm, Chemistry of the Solid–Water Interface, Wiley Interscience, New York, 1992.
[19] X. Zhu, M. Elimelech, Fouling of reverse osmosis membranes by aluminium oxide colloids, J. Environ. Eng., 121 (1995) 884–893.
[20] S. Srisurichan, R. Jiraratananon, A. Fane, Mass transfer mechanisms and transport resistances in direct contact membrane distillation process, J. Membr. Sci., 277 (2006) 186–194.
[21] S. Walczak, N. Cerpa, Artificial Neural Networks, R.A. Meyers, Ed., Encyclopedia of Physical Science and Technology, 3rd ed., Academic Press, San Diego, CA, 2003, pp. 631–645.
[22] V.N. Delgrange, N. Cabassud, M. Cabassud, L. Durand-Bourlier, J.M. Laine, Neural networks for prediction of ultrafiltration transmembrane pressure: application to drinking water production, J. Membr. Sci., 150 (1998) 111–123.